Computational Modeling of a Trebuchet

Jeremy Fleishhacker, Charlie Hall, Henry Sottrel, and Ben Turner
Carleton College, Department of Physics, Northfield,MN 55057
(Dated: March 15, 2021)

In this study, a trebuchet with a hinged counterweight and rotating projectile sling was analyzed. Since the system cannot be solved analytically, Lagrangian mechanics were used to create a computational model of a trebuchet launch. We investigated the following areas using this model: the constraint forces which act during the throw, the launch time and fulcrum length which maximize the projectile range, and the increase in efficiency provided by the addition of wheels.

I. TREBUCHET BACKGROUND

The trebuchet is a powerful medieval siege engine which was widely employed to break castle walls by throwing heavy projectiles. This weapon is interesting to analyze using the tools of mechanics because it is a complex system with multiple moving parts. Its predecessor, the catapult, relied on a single rotating fulcrum with a counterweight and projectile on opposite ends. This means that a catapult can functionally be reduced to a single rigid body rotating due to gravity, which makes it relatively simple to model. In contrast, the trebuchet, which typically has a hinged counterweight and a projectile sling which is free to rotate[5], is a much more complex system.

The addition of the counterweight hinge and the movable sling made trebuchets much more efficient than catapults[1]. However, the expansion of the degrees of freedom of the motion also complicates the dynamics of the system. Unlike the catapult, we should not generally expect to be able to find an simple solution for the trebuchet's equations of motion[1].

While this makes it a difficult system to model, it also makes it a very interesting one. As a real-world example of a system with very complex dynamics, the trebuchet is an interesting system to solve using the tools of Lagrangian mechanics and modern computers, which make real-time simulations of similar systems possible.

While medieval engineers likely optimized the range of their trebuchets through trial and error, we can attempt to optimize some aspects of our virtual trebuchet, such as the length of the throwing arm and the angle at which the projectile is released, using more rigorous methods. By running simulations with different values of some parameter and noting the efficiency of the trebuchet in each simulation, we can find the value where efficiency is maximized. Most medieval trebuchets also had wheels, and a computational simulation allows us to determine how much extra efficiency, if any, the trebuchet system will gain from adding wheels.

Other groups have done work in the area of modeling trebuchet dynamics. While many of our methods were similar to those of Denny[1], the initial conditions of our setup, with the throwing arm pointed in the direction of the launch and the counterweight pointed almost straight up, is not covered in his work.

II. OUR SYSTEM

The computational model we created was based off of the VEX Robotics Trebuchet.

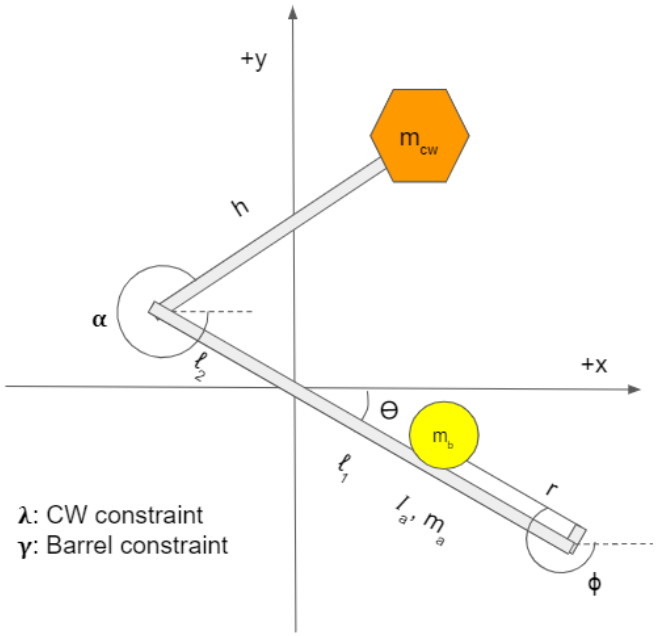

FIG. 1: Diagram of Trebuchet system with labeled variables. The fulcrum is located at the origin.

In our initial evaluation of the system, we determined that there are three degrees of freedom—the angle θ of the throwing arm, the angle α of the counterweight arm, and the angle ϕ of the sling (see Fig. 1). All three of these angles are absolute with respect to the horizontal. There are two constraint forces —the normal force of the main arm on the counterweight arm which prevents it from swinging in, and the normal force on the projectile which prevents it from swinging through the main arm.

We assumed that the projectile acts as a point mass, that the main arm can be modeled as a rod of uniform density, and that the mass of the counterweight arm is concentrated entirely at its end. We also assumed that the sling to which the projectile is attached acts as a rigid, massless rod. Finally, we assumed that the components of the trebuchet do not experience friction or air

resistance. These assumptions simplify our Lagrangian while keeping the most important properties of the system intact.

Our initial Lagrangian is given by

$$L = T - U + \lambda G_1 + \gamma G_2, \tag{1}$$

for kinetic and potential energies T and U, Lagrange multipliers λ and γ, and constraint functions G_1 and G_2. The kinetic energy T is

$$T = \frac{1}{2}(m_b(\dot{x}_b^2 + \dot{y}_b^2) + I_a\dot{\theta}^2 + m_{cw}(\dot{x}_{cw}^2 + \dot{y}_{cw}^2)), \tag{2}$$

where (x_b,y_b) is the position of the barrel, (x_{cw},y_{cw}) is the position of the counterweight, and (x_a,y_a) is the position of the center of mass of the throwing arm. m_b, m_{cw}, and m_a are the masses of the barrel, counterweight, and throwing arm respectively. I_a is the moment of Inertia of the throwing arm.

The potential energy U is

$$U = m_{cw}gy_{cw} + m_bgy_b + m_agy_a, \tag{3}$$

and the transformations from Cartesian coordinates to the generalized coordinates are

$$x_b = l_1\cos(\theta) + r\cos(\phi) \tag{4a}$$
$$y_b = -l_1\sin(\theta) - r\sin(\phi) \tag{4b}$$
$$x_{cw} = -l_2\cos(\theta) + h\cos(\alpha) \tag{4c}$$
$$y_{cw} = l_2\sin(\theta) - h\sin(\alpha) \tag{4d}$$
$$y_a = -\frac{l_1 - l_2}{2}\sin(\theta). \tag{4e}$$

For the moment of inertia of the throwing arm I_a, the equation is[1]:

$$I_a = \frac{1}{3}m_a(\frac{l_1^3 + l_2^3}{l_1 + l_2}). \tag{5}$$

The constraint equations on the early motion of the trebuchet are given by:

$$G_1 = \theta - \phi + \phi_0 \tag{6}$$
$$G_2 = \theta - \alpha + \alpha_0., \tag{7}$$

where $\phi_0 = \phi[0]$ and $\alpha_0 = \alpha[0]$.

We took measurements of the physical model and scaled them up for parameters in the computational model to obtain results on the order of magnitude of historical trebuchets, while still being able to make qualitative conclusions regarding the VEX model. The length of the counterweight arm is h, the sling length is r, and the throwing arm has component l_1 on the sling side of the fulcrum and l_2 on the counterweight side.The parameters that were used in the simulations are given in Tab. I.

Constants		Constants	
l_1 (m)	10	m_a (kg)	1000
l_2 (m)	4	h (m)	10
m_b (kg)	60	r (m)	6
m_{cw} (kg)	3000	g (m/s^2)	9.81

TABLE I: Table of Constants. g the acceleration due to gravity. The masses are scaled up from our physical measurements by a magnitude of 10,000 and the lengths are scaled up by a magnitude of 50.

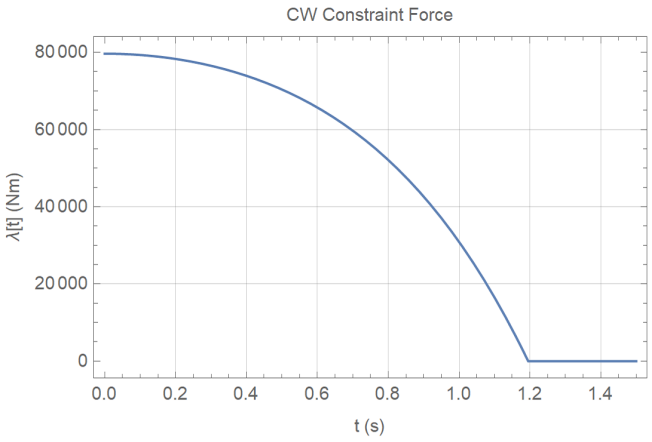

FIG. 2: Constraint force on the Counterweight arm vs Time.

III. MODELING CONSIDERATIONS

By numerically solving the system of differential equations obtained from the Euler-Lagrange equations using the Mathematica command NDSolve over the relevant period of time, we obtained plots for the two relevant constraint functions of time. Based on these plots, the λ equation, corresponding to the constraint force on the counterweight arm, is the first constraint to hit zero. After integrating up to the point at which the first constraint reached zero, we removed that constraint from the system of differential equations and solved a new system of equations with initial conditions determined using the first solution. We repeated this process with the second constraint to find piecewise functions that describe the angles and constraint forces as functions of time.

The constraint force on the counterweight arm during the initial swing appears to be roughly quadratic, starting at a high initial value and decreasing like a parabola to zero. During this first part of the swing, the system is just one rigid mass rotating about a fixed point due to a gravitational torque.

During the part of the swing when both constraint forces act on the system, γ, the constraint force on the barrel behaves similarly to the force on the counterweight, but in the opposite direction. This force starts at

a negative value of high magnitude and increases like a parabola. Interestingly, since the constraint force on the counterweight goes to zero before the force on the barrel does, there is an interval of time in which the barrel constraint force is acting on the system, but the counterweight constraint force is not. In this region, γ approaches zero nearly linearly with time, in contrast to the curve which described its behavior previously. Physically, we could interpret this change in the behavior of the barrel constraint as the outswing of the counterweight arm jerking the main arm out and causing the projectile to swing out more quickly.

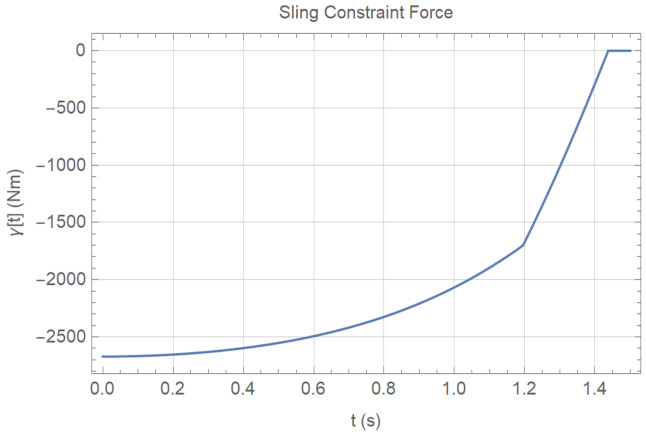

FIG. 3: Constraint force on the Barrel vs Time.

We incorporated a third constraint force which acts on the main arm of the trebuchet once it is pointed vertically upward. This force models the fact that in our actual apparatus, the main arm is not free to swing further once it reaches the top of its arc. However, because the projectile is always launched before the main arm reaches the top of its swing, this constraint force does not at all affect the trebuchet's range.

IV. LAUNCH ANGLE OPTIMIZATION

An important historical advantage of the medieval trebuchet was its range. A crucial factor in determining the range is the projectile's launch angle. From introductory physics, we know the optimal angle relative to the horizontal to be 45° or $\frac{\pi}{4}$ radians. We wanted to explore whether our trebuchet achieved maximum range for a 45° launch angle.

We chose to determine the angle of release by finding the optimal time of launch and using the x and y velocities of the projectile at that time. We wanted to optimize the total distance the barrel traveled in the x-direction until it returned to $y = 0$ after release. In order to isolate the time-distance relationship, we kept the other conditions constant, whose values can be found in Table I.

We used Mathematica to simulate our trebuchet launching at the different times. With a time step of 0.005s, we recorded the distance traveled by the projectile for an estimated time range of release, for which the data can be seen in Fig. 4 below.

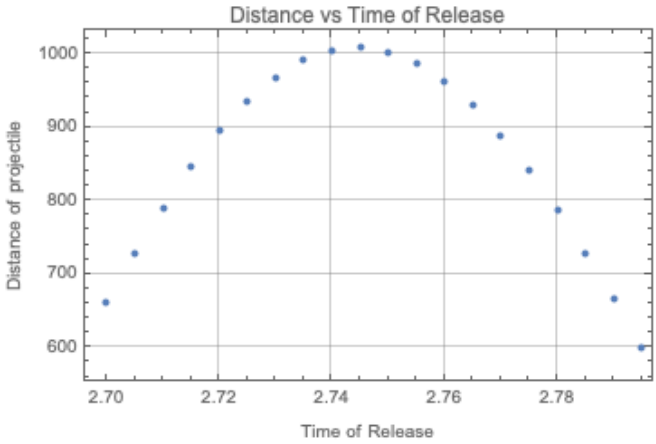

FIG. 4: Distance vs Time of Release. This is for the parameters state in Tab. I, and with a time step of 0.01s.

Our results determined the optimal time of release without drag to be 2.745s. Using the piece-wise function for ϕ, we were able to determine the angle of release to be 585° or 10.2 radians. This aligns with what we expected for the projectile angle. Since ϕ is the orientation of sling, we would expect the velocity of release to be perpendicular to ϕ. Thus, when adding the 90° to find the angle of the projectile velocity at release, we find it to be 45° above the positive horizontal, which we defined as absolute 0 for all angles. This confirms that 45° is the optimal angle for our system. If this had not been the case, we would have expected a higher speed at the new optimal angle that counterbalances the lack of 45° optimization. This tells us that the designers of the Vex trebuchet were careful to create a system that reached peak velocity at the best angle of release.

Since the above analysis was drag-less, it is important to also address whether the same angle applies to a physical case with drag. Using the same process as above, we found the optimal angle of release for differing drag environments as seen in Tab. II.

As a limitation of our code, we were only able to simulate drag for the projectile after release. This caused our trebuchet to be in a "bubble" in which it operates without drag. This affects our results particularly for Venus, as the extremely thick atmosphere stops the projectile very quickly. Thus, we see such a significantly smaller angle of release since it will go farther without drag if it stays in the "bubble" for longer. We notice that the Moon, Mars, and Earth are all close to the ideal 45°. Due to the large size of the projectile, the drag force plays a significant role in the motion after release. This is especially so on Venus, since the density of the atmosphere is so large. In conclusion, we see that as drag increases, the

Celestial Body	ψ	ρ (m/kg^3)	g (m/s^2)
Moon	45°	0	1.62
Mars	46.9°	0.02	3.71
Earth	41.5°	1.2	9.81
Venus	14.9°	65	8.87

TABLE II: Optimal Angle of Release for Different Celestial Bodies. Each celestial body has a different optimal angle ψ made above the horizontal, with conditions ρ of atmospheric density and g the acceleration due to gravity in each environment.

optimal angle of launch generally decreases. The only exception to this is Mars, which would be an interesting further source of study. When humans reach these locations, they should note that the Vex trebuchet does not provide the projectile the largest speed at the optimal angle of release anymore. It would need an adjustment to be the most efficient for that environment.

V. FULCRUM OPTIMIZATION

When constructing a trebuchet, it is important to consider where to place the fulcrum along the main beam to make the machine most efficient. This placement will depend on the system. The firing speed is a good measure of optimization since it is a display of the power of the system, and the distance traveled by the projectile depends on launch speed. Computationally, we wanted to determine what lever arm ratio would give the maximum firing velocity.

The scaled-up throwing arm of the trebuchet was 14 m in length. Using the NDSolve function mentioned above, different values of l_1 were looped through to find equations of motion for different fulcrum positions. Assuming the optimum launch angle of 45°, the speed of the barrel was calculated when the launch point was reached. The results were plotted in Fig. 5.

Our original computational model (based on the physical model) had $l_1 = 10$ m, where the launch speed was calculated as 99.4 m/s. The maximum speed was calculated to be 100.55 m/s when $l_1 = 9.91$ m. So, the physical model seems to be nearly optimized for launch speed based on the measurements we made. A 9.91 m l_1 leads to a lever arm ratio of 2.42 : 1 for $l_1 : l_2$, just less than the physical model's ratio of 2.5 : 1 for $l_1 : l_2$.

Some interesting parts of the plot are the regions where the launch speed is zero. Launch speed is zero when $l_1 = 10.3$ m, which seems to be an error in the computation since the other points in the middle of the plot follow a clear trend. However, when $l_1 < 9.9$ m, the behavior of the launch speed changes abruptly and becomes unpredictable. What happens physically when $l_1 < 9.9$ m is the trebuchet falls backwards. This region is not fully shown in the plot, but there is no general trend for the region, as sometimes the projectile will fire in the backwards direction with a high speed, but sometimes the motion will be awkward, causing a slow speed.

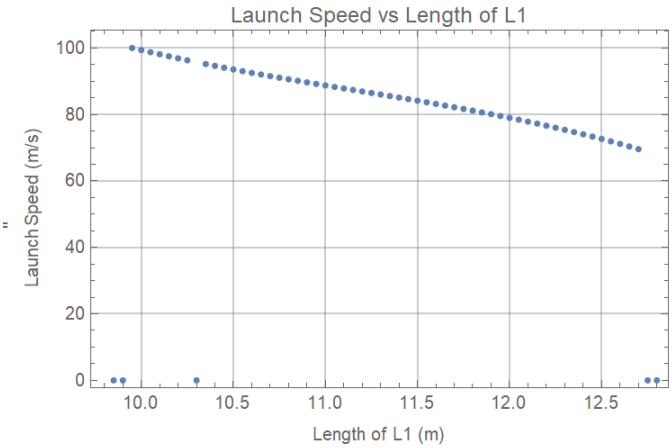

FIG. 5: Launch speed against l_1, the length of the throwing arm component on the sling slide of the trebuchet.

A hypothesis for the unexpected behavior is that it is due to the unique set-up of the system where the counterweight starts hanging on the same side as the projectile. If l_1 is too short, the counterweight will start past the pivot point and fall the wrong direction. The physical model cannot fall backwards due to the trebuchet locking into its starting position, but the computational model does not take this into account.

A similar behavior occurs when $l_1 > 12.7$ m; the launch speed is zero. This also must be a threshold of the parameter that our system struggles with. Due to the set-up of the counterweight physically, the trebuchet's motion must not be fluid.

The general form of the curve is linear-like and downwards-sloping, and the curve stretches from values of l_1 just under 10 m to around 12.7 m. This is the range of l_1 that produces the expected motion of the trebuchet. In this region as the length of l_1 increases, the launch speed decreases.

Denny[1] determined that the optimum lever arm ratio for a similar system was within $3 \leq \frac{l_1}{l_2} \leq 5$. This tells us that a range of values is possible depending on the system, making our 2.42 : 1 ratio seem reasonable due to the unique elements of this model. The VEX model seems to be nearly optimized, having a fulcrum location that is almost at the maximum launch speed but without the fear of having the machine launch improperly with the counterweight falling the wrong way.

VI. ADDITIONAL GENERALIZED COORDINATES

Our design is not the only way to construct a trebuchet. Medieval engineers conceived of other systems

which introduced more degrees of freedom to achieve more efficient motion. One such system involved the addition of wheels to the trebuchet, effectively introducing a horizontal translational degree of freedom to the system. To explore this setup, we introduced a generalized coordinate x_p which tracks the horizontal position of the trebuchet pivot point. As before, the full Lagrangian is given by Eq. 1. Since we can no longer regard the pivot point as fixed, we must account for the translational motion of the throwing arm center of mass and the rotational motion of the arm about its center of mass, so the kinetic energy in Cartesian coordinates becomes

$$T = \frac{1}{2}(m_{cw}(\dot{x}_{cw}^2+\dot{y}_{cw}^2)+m_b(\dot{x}_b^2+\dot{y}_b^2)+m_a(\dot{x}_a^2+\dot{y}_a^2)+I_a\dot{\theta}^2). \tag{8}$$

I_a is the moment of inertia of the throwing arm around its center of mass. Since we modeled the throwing arm as a thin rod, this is given by

$$I_a = \frac{1}{12}m_a(l_1+l_2)^2. \tag{9}$$

The potential energy in Cartesian coordinates is given by Eq. 3 as before. We converted the Lagrangian into generalized coordinates θ, ϕ, α, and x_p. The first three coordinates are the angles we used to model the motion of the fixed trebuchet, and the last coordinate is introduced to account for the additional horizontal degree of freedom. We used Eqs 4b, 4d, and 4e to convert the vertical coordinates and used

$$x_b = x_p + l_1\cos\theta + r\cos\phi, \tag{10a}$$

$$x_{cw} = x_p - l_2\cos\theta + h\cos\alpha, \tag{10b}$$

$$x_a = x_p + \frac{l_1-l_2}{2}\cos\theta, \tag{10c}$$

to convert the horizontal coordinates. We assumed Eqs. 6 and 7 as before to constrain the early motion of the trebuchet.

As with the fixed trebuchet, we numerically solved the Euler-Lagrange equations corresponding to Eq. 1 in three steps. We integrated with both constraints present in the Lagrangian until λ became zero. Then, we integrated with only constraint G_2 until γ became zero. We completed the numerical simulation with both constraints removed.

We expected the performance of the rolling trebuchet to be markedly improved compared to the fixed apparatus. This is because the horizontal degree of freedom enables the counterweight to fall in a straighter line, giving more kinetic energy to the projectile at the end of the sling. Moreover, the entire construction may be moving forward as the projectile is launched, thus increasing its speed at launch. Since both our fixed and rolling systems have the same total energy and the energy is conserved, we used the energy ratio R of the kinetic energy of the projectile at launch $T_{b,l}$ to the total energy E as an efficiency metric. For a time of launch t_l, R is given by

$$R = \frac{T_{b,l}}{E} = \frac{\frac{1}{2}m_b(\dot{x}_b[t_l]^2+\dot{y}_b[t_l]^2)}{T+U}. \tag{11}$$

We determined t_l as the time at which the projectile velocity reaches the ideal launch angle, 45°. We obtained $R_f = 1.42$ for the fixed trebuchet and $R_r = 1.83$ for the rolling apparatus. Note that these values are physical since our choice of coordinates permits negative potential energies. These results confirm our predictions; the rolling trebuchet projectile had about 1.3 times the kinetic energy of the fixed system projectile. This corresponds to a speed difference of 13 m/s. So, the rolling trebuchet performed better than the fixed system.

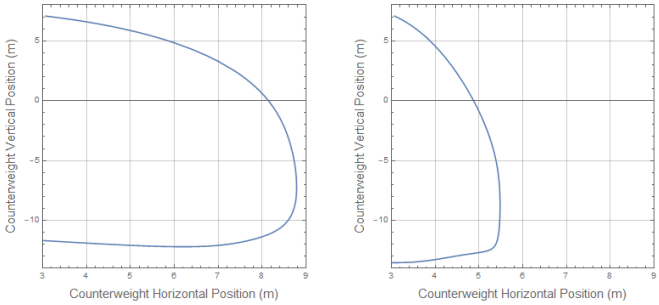

(a) Fixed Trebuchet (b) Rolling Trebuchet

FIG. 6: Trajectory of the counterweight during its initial swing for (a) the fixed trebuchet and (b) the rolling trebuchet. The horizontal axis is the horizontal position of the counterweight in meters and the vertical axis is the vertical position of the counterweight in meters. The counterweight swings out further horizontally for the fixed trebuchet.

To compare the motion of the rolling and fixed systems more thoroughly, we analyzed the trajectory of the counterweight during its initial swing. Figure 6 shows the results. As expected, the counterweight on the fixed trebuchet swings out 3.3 meters further than it does in the rolling apparatus, for a total of 6.6 meters of additional horizontal distance traveled. The rolling of the system in Fig. 6b thus enables the counterweight to travel in a straighter line. As a result, less energy is wasted on the rotation of the counterweight and the projectile gains more kinetic energy.

We also explored possible values of R for different t_l. As evident in Fig. 7a, the maximum energy ratio occurs approximately at the time corresponding to the ideal launch angle (red gridlines). This indicates that the fixed system is behaving optimally in the sense that the maximum possible speed of the projectile coincides with the ideal launch angle. As such, the fixed trebuchet fires the projectile with the maximum possible range given its design. Figure 7b, on the other hand, shows that, for the rolling apparatus, the projectile reaches its maximum kinetic energy after the time corresponding to the ideal launch angle. Hence, the maximum possible speed of the projectile does not coincide with the ideal launch angle. In this regard, the rolling trebuchet is not optimally designed; the projectile reaches the ideal launch angle too early to benefit from the full power of the trebuchet.

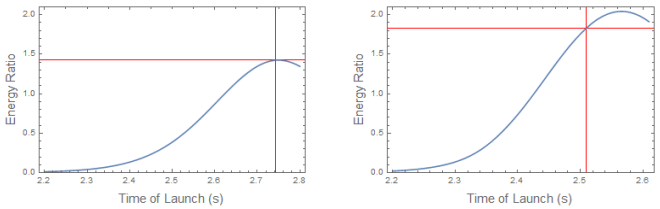

(a) Fixed Trebuchet (b) Rolling Trebuchet

FIG. 7: Ratio of projectile kinetic energy to total energy at different launch times for (a) the fixed trebuchet and (b) the rolling trebuchet. The horizontal axis is the time of launch t_l in seconds and the vertical axis is the energy ratio, R. The red gridlines represent the launch time corresponding to the ideal launch angle, 45°, and the energy ratio at this time.

Although the rolling system performs better than the fixed system, it does not take full advantage of its additional power. Simply adding wheels to any trebuchet may improve performance but does not guarantee optimal performance. Designing the system as a rolling trebuchet from the ground up—in order to ensure that the maximum projectile kinetic energy coincides with the ideal launch angle—would maximize the possible firing range. Modern engineers have produced even more efficient trebuchet designs, which are not analyzed in this paper. One example is the floating arm trebuchet, a five degree-of-freedom system which incorporates a main arm without a fixed pivot point and a counterweight that falls downward in a perfectly straight line[4]. This construction is highly efficient since the full potential energy of the counterweight is applied to increase the projectile kinetic energy rather than the rotational kinetic energy of the counterweight. With clever system design, engineers can obtain significantly better performance than the classic fixed trebuchet using these higher degree-of-freedom systems.

VII. DISCUSSION

In summary, we were able to answer our questions using the computational model we constructed. We found that the constraint forces are interdependent in that removing one constraint significantly changes the behavior of the other constraint. The optimal launch angle taking into account that the speed of the projectile might be changing at potential launch angles, assuming no air resistance, was 45°, as the kinetic energy of the projectile is highest at that point. We found an optimal lever arm ratio to be 2.42:1, which was similar to the lever arm ratio of our physical trebuchet. Finally, we found that adding wheels to our simulated trebuchet improved its efficiency, but that this system does not behave optimally for a rolling weapon. Ideally, we would design our rolling apparatus in such a way that the maximum velocity of the projectile is reached at the 45° ideal launch angle.

Since we modeled no non-conservative forces, the total energy should remain constant over time. We evaluated the computational error by measuring the maximum deviation of the energy from the initial value over time. For our simulations of both the fixed and rolling trebuchets, we obtained a deviation of less than 1 J, which corresponds to a percent error of less than 0.0005%. Thus, we are quite confident that computational error had little to no effect on our results.

Based on the optimal parameters we calculated computationally and the actual parameters of the VEX trebuchet on which our computational model was grounded, the engineers of the VEX trebuchet seem to have put a lot of thought into their design. Many of the parameters of that trebuchet are optimized or near-optimized.

Our method of modeling the trebuchet proved effective, not just because we were able to produce accurate results, but because our code proved versatile enough that we were able to use the same base code with modifications to investigate a wide variety of questions about our system. This made the task of investigating several different questions independently much more viable. Additionally, there are many questions left unanswered which this code could be used to investigate.

ACKNOWLEDGMENTS

We would like to thank Jay Tasson for funding this project, giving feedback on our work, and supporting us along the way.

[1] Mark Denny, "Siege engine dynamics", Eur, J, Phys. 26 561-577 (2005)
[2] G. Annoscia, M. Bici, F. Campana, and L. De Lellis, "Virtual prototyping of medieval weapons for historical reconstruction of siege scenarios starting from topography and archaeological investigations", IOP Conf. Series: Materials Science and Engineering 364 (2018) 012098
[3] Zenos Christo, "Analysis of the optimum fulcrum position of a trebuchet", Phys. Educ. 52 (2017) 013010
[4] Eric Constans, "A Lagrangian Simulation of the Floating-Arm Trebuchet", (2017), The College Mathematics Journal, 48:3, 179-187
[5] Paul E. Chevedden, "The Trebuchet", Scientific American , Vol. 273, No. 1 (1995), pp. 66-71
[6] L. Partridge, D. Cornwell, T. Sewart, D. Armengol Arcas, and C. Wilcox, "P1 2 Using Trebuchets for Lunar Satellites", Journal of Physics Special Topics (2019)

Appendix A: Division of Work

Jeremy: I was the trebuchet master, so I played a significant role in building the physical model. Henry, Ben, and I wrote the simulations in Mathematica and programmed the animations. I focused on the question of how adding wheels to the model affects the motion. This was a computational exploration, and I altered the original simulation code by adding a fourth generalized coordinate to complete the analysis. I also obtained the computational error for our simulations.

Henry: I organized the slides for our report and planned the general structure of our presentation. Answering the questions, I focused on analyzing the constraint forces which act on the counterweight arm and sling during the swing, figuring out how they change with time, and how to deal with some constraints 'vanishing' after they hit zero the first time. I also worked on setting up the manipulate commands to animate our simulate trebuchet.

Ben: I was the code keeper, so I directed efforts on simulating our system. Both Henry and Jeremy contributed a lot to the code too, so together we were able to successfully simulate our complex system. I also helped create code specific to optimization questions, including those for angle and fulcrum position. Using this code I investigated optimization of different aspects of the trebuchet with Charlie, and eventually decided to look into the angle of release.

Charlie: My main efforts were with this report and in the general organization of things, including the presentation slides. I was the paper editor. I was actively a part of all things besides the designing of the baseline Mathematica Notebook. I took the lead on the optimization of the fulcrum position question, but Ben was a big help with the computation of the question and I received some advice from the others.